Nanostructured Materials for Advanced Li-Ion Rechargeable Batteries

Alternative energy being developed through electrochemical means.

YING WANG AND GUOZHONG CAO

Digital Object Identifier 10.1109/MNANO.2009.932418

THE RECENT INCREASE IN demand for oil, associated with oil price increase, and environmental issues are continuing to exert pressure on an already stretched world energy infrastructure. One alternative energy/power source under serious consideration is electrochemical energy, since this energy production is designed to be more sustainable and more environmentally benign. The lithium-ion (Li-ion) battery is the representative system for such electrochemical energy storage and conversion. It has been intensively studied for use as power supplies of electric vehicles (EVs) and hybrid electric vehicles (HEVs). High energy and high power densities are required for such devices. Li-ion batteries are attractive power-storage devices owing to their high energy density [1]. However, their power density is relatively low because of a large polarization at high charging–discharging rates. This polarization is caused by slow lithium diffusion in the active material and increases in the resistance of the electrolyte when the charging–discharging rate is increased. To overcome these problems, it is important to design and fabricate nanostructured electrode materials that provide high surface area and short diffusion paths for ionic transport and electronic conduction.

Intercalation electrodes in batteries are electroactive materials and serve as a host solid into which guest species are reversibly intercalated from an electrolyte. The area of cathodes is much less developed than anodes [2]. Details on Li-ion battery cathode materials can be found in recent reviews by Whittingham et al. [3], [4]. There are two categories of cathode materials. One is layered compounds with anion close-packed lattice; transition metal cations occupy alternate layers

1932-4510/09/$25.00©2009IEEE

between the anion sheets, and Li ions are intercalated into the remaining empty layers. $LiTiS_2$, $LiCoO_2$, $LiNi_{1-x}Co_xO_2$, and $LiNi_xMn_xCo_{1-2x}O_2$ belong to this group. The spinels with the transition metal cations ordered in all the layers can be considered to be in this group as well. This class of materials has the inherent advantage of higher energy density (energy per unit of volume) owing to their more compact lattices. The other group of cathode materials has more open structures, such as vanadium oxides, the tunnel compounds of manganese oxides, and transition metal phosphates (e.g., the olivine $LiFePO_4$). These materials generally provide the advantages of better safety and lower cost compared to the first group.

This article aims to give a concise and useful survey of recent progress on synthesis and characterizations of nanostructured cathode materials for Li-ion batteries, taking vanadium oxide as a model system. Electrochemical Li intercalation occurs together with compensating electrons, leading to the formation of vanadium bronzes as follows:

$$V_2O_5 + xLi^+ + xe^- \Leftrightarrow Li_xV_2O_5. \quad (1)$$

It is easy to understand that nanostructured cathode electrodes offer improved energy storage capacity and charge or discharge kinetics, as well as better cyclic stabilities because of their huge surface area for Faradaic reaction, and short distance for mass and charge diffusion, as well as the added freedom for volume change accompanied to Li-ion intercalation and discharge.

NANOSTRUCTURED VANADIUM OXIDES

Vanadium oxide is a typical intercalation compound as a result of its layered structure. For Li-ion intercalation applications, vanadium oxide offers the essential advantages of low cost, abundant source, easy synthesis, and high energy densities. Orthorhombic crystalline V_2O_5 consists of layers of VO_5 square pyramids that share edges and corners [5]. To obtain electrodes for battery cell testing, the synthesized freestanding vanadium oxide nanostructures (e.g., nanorolls, nanobelts, and nanoribbons) are usually mixed with conductive elements such as carbon black; the mixtures are then pressed into pellets and are used as electrodes. For ordered nanostructures such as arrays of nanorods, nanotubes, and nanocables, they are synthesized on the conductive substrates and can be used directly for battery cell testing.

VANADIUM OXIDE NANOROLLS, NANOBELTS, AND NANORIBBONS

To date, there are a large number of publications on nanostructures of vanadium oxides. Pioneering work on the synthesis and electrochemical properties of vanadium oxide nanorolls has been carried out by Spahr and coworkers [6]. In their synthesis, a combination of sol–gel reaction and hydrothermal treatment of vanadium oxide precursor is conducted in the presence of an amine that acts as structure-directing template [7]. The resultant nanoroll is either constructed in closed concentric cylinders (nanotubes) or formed by scrolling one or more layers (nanoscrolls). If amine is replaced by ammonia during the hydrolysis step, a new type of vanadium oxide nanoroll (nanotube) with alternating interlayer distances is yielded [8]. Such a unique structure is first observed in a tubular phase.

Compared to other tubular systems, the vanadium oxide nanorolls are especially interesting because they possess four different contact regions, that is, tube opening, outer surface, inner surface, and interstitial region. VO_x nanorolls can intercalate a variety of molecules and ions reversibly without change in the crystalline structure. The Li intercalation capacities have been found up to 200 mAh/g; however, there is structural breakdown during redox cycles and degradation in cycling performance because of the morphological flexibility. The cyclic voltammetry measurements show that the well-ordered nanorolls behave closely to classic crystalline vanadium pentoxide, while the defect-rich nanorolls have electrochemical behavior similar to that of sol–gel-prepared hydrated vanadium pentoxide materials. The specific capacity of defect-rich nanorolls (340 mAh/g) is higher than that of the well-ordered nanorolls (240 mAh/g) under comparable conditions.

Hydrothermal synthesis is another powerful tool to transform transition metal oxides into high-quality nanostructures, and nanostructured vanadium oxides in different morphologies can be produced via this procedure. Examples include long, belt-like nanowires growing along the [010] direction [9] and new types of belts exhibiting a boomerang shape [10]. The structure of these nanobelts is unique in that it originates from twinning along the [130] direction, which is the first observation of twins within individual nanosized crystals. Vanadium pentoxide nanobelts have been prepared to be used as highly selective and stable ethanol sensor materials by acidifying ammonium metavanadate followed by hydrothermal treatment [11]. In a separate report, $V_2O_5 \cdot nH_2O$ crystalline sheets, the intermediate products between nanobelts and nanowires, are fabricated hydrothermally using V_2O_5, H_2O_2, and HCl [12]. Nevertheless, the intercalation properties of these vanadium oxide nanobelts or nanosheets are not further investigated.

More recently, Li et al. have studied the synthesis and electrochemical behavior of orthorhombic single-crystalline V_2O_5 nanobelts [13]. The V_2O_5 nanobelts with widths of 100–300 nm, thicknesses of 30–40 nm, and lengths up to tens of micrometers are obtained by hydrothermal treatment of aqueous solutions of V_2O_5 and H_2O_2. The authors propose a dehydration–recrystallization–cleavage mechanism for the formation of V_2O_5 nanobelts. A high initial discharge capacity of 288 mAh/g is found for the V_2O_5 nanobelts in a voltage range of 4.0–1.5 V; subsequently, the capacity decreases to 191 mAh/g for the second cycle and then remains steady for the next four cycles. Apart from anhydrous crystalline V_2O_5 nanobelts, $V_2O_5 \cdot 0.9H_2O$ nanobelts and $V_2O_5 \cdot 0.6H_2O$ nanorolls are synthesized with hydrothermal treatment of NH_4VO_3 in the presence of different acids [14]. The $V_2O_5 \cdot 0.9H_2O$ nanobelts are tens of micrometers long, 100–150 nm wide, and 20–30 nm thick. The $V_2O_5 \cdot 0.6H_2O$ nanorolls are half-tube nanostructured as

a result of incomplete scrolling. It is interesting to note that $V_2O_5 \cdot 0.6H_2O$ nanorolls show higher intercalation capacity (253.6 mAh/g) than $V_2O_5 \cdot 0.9H_2O$ do nanobelts (223.9 mAh/g) under a current density of 0.6 mA/g, which can be ascribed to the higher surface area and lower water content of nanorolls. Furthermore, the capacities of nanorolls and nanobelts increases to 287.8 and 307.5 mAh/g, respectively, after annealing and dehydration of these nanostructures, which suggests the significant effect of water content on the electrochemical behavior.

Size is another factor affecting the electrochemical property. In this regard, Cui and coworkers prepared V_2O_5 nanoribbons and investigated the dependence of the electrochemical property on the width and thickness of nanoribbons by studying the chemical, structural, and electrical transformations of V_2O_5 nanoribbons at the nanostructured level [15]. They found that transformation of V_2O_5 into the ω-$Li_3V_2O_5$ phase takes place within 10 s in thin nanoribbons, and the efficient electronic transport can be maintained to charge ω-$Li_3V_2O_5$ nanoribbon within less than 5 s. Therefore, it is suggested that Li diffusion constant in nanoribbons is faster than that in bulk materials by three orders of magnitude, leading to a remarkable enhancement in power density (360 °C). It can be concluded that Li-ion batteries based on nanostructured vanadium oxides have not only higher energy density but also higher power density and thus will find applications in EVs and HEVs.

ORDERED ARRAYS OF VANADIUM OXIDE NANORODS, NANOTUBES, AND NANOCABLES

Martin and coworkers have reported a series of studies on polycrystalline V_2O_5 nanorod arrays. They used a template-based method by depositing triisopropoxyvanadium(V) oxide (TIVO) into the pores of polycarbonate filtration membranes followed by removal of membranes at high temperature [16]. The V_2O_5 nanorod arrays deliver three times the capacity of the thin film electrode at a high rate of 200 °C and four times the capacity of the thin-film control electrode above 500 °C. After that, Li et al. achieved improved volumetric energy densities of V_2O_5 nanorod arrays by chemically etching the polycarbonate membrane to increase its porosity prior to template synthesis [17]. In the latest work of Sides and Martin, V_2O_5 nanorods of different diameters were prepared, and their electrochemical properties at low temperature were compared [18]. V_2O_5 nanorods with nanometer-sized diameters (e.g., 70 nm) deliver dramatically higher specific discharge capacities at low temperature than V_2O_5 do nanorods with micrometer-sized diameters. Thus, Li-ion battery electrodes composed of nanosized material meet the low-temperature performance challenge, because nanomaterials alleviate the problems of slow electrochemical kinetics and the slow diffusion by offering high surface area and short diffusion distance.

Synthesis and electrochemical properties of single-crystal V_2O_5 nanorod arrays were first reported by Cao, Wang and coworkers [19]–[21]. They have utilized a template-based electrode position method by depositing V_2O_5 into pores of polycarbonate templates, with the assistance of electric field from three different types of solutions or sol, i.e., VO^{2+} solution, VO^{2+} solution, and V_2O_5 sol. Figure 1(a) and (c) show transmission electron microscope (TEM) images of a V_2O_5 nanorod and selected area electron diffraction pattern, which clearly demonstrated the single-crystalline nature or, at least, well-textured nature of the grown nanorods with a [010] growth direction for nanorods grown from both routes. Figure 1(b) and (d) also show high-resolution TEM images of

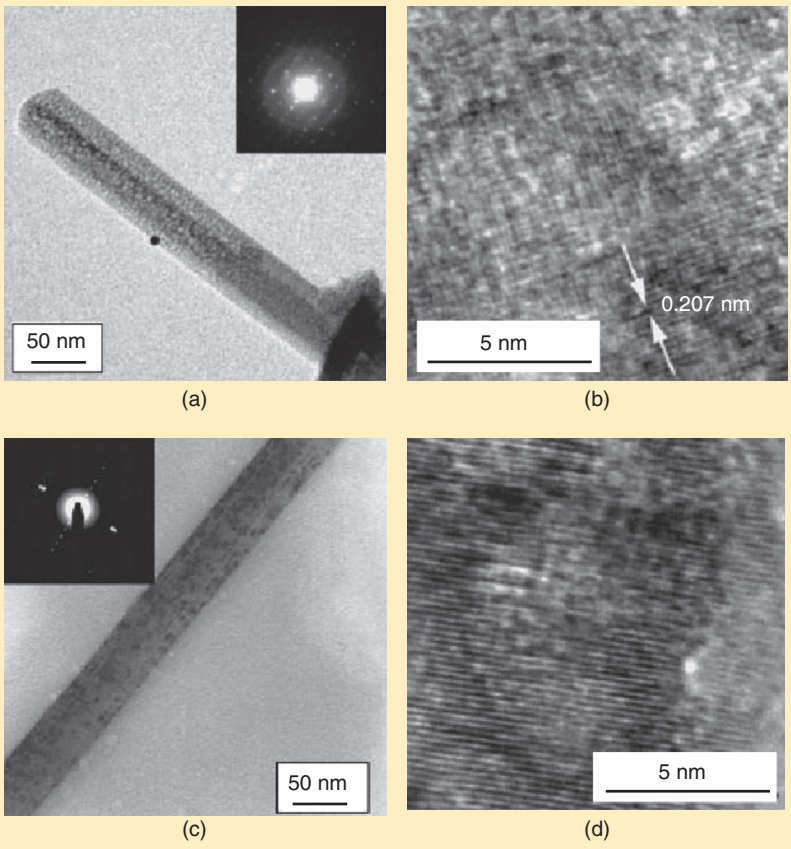

FIGURE 1 (a) TEM image and selected area electron diffraction pattern of a V_2O_5 nanorod prepared from template-based electrochemical deposition from $VOSO_4$ solution. (b) High-resolution TEM image of the V_2O_5 nanorod in (a). The spacing of the fringes was measured to be 0.207 nm. (c) TEM image and selected area electron diffraction pattern of a V_2O_5 nanorod prepared from template-based electrophoretic deposition from V_2O_5 sol. (d) High-resolution TEM image of the V_2O_5 nanorod in (c). The spacing of the fringes was measured to be 0.208 nm.

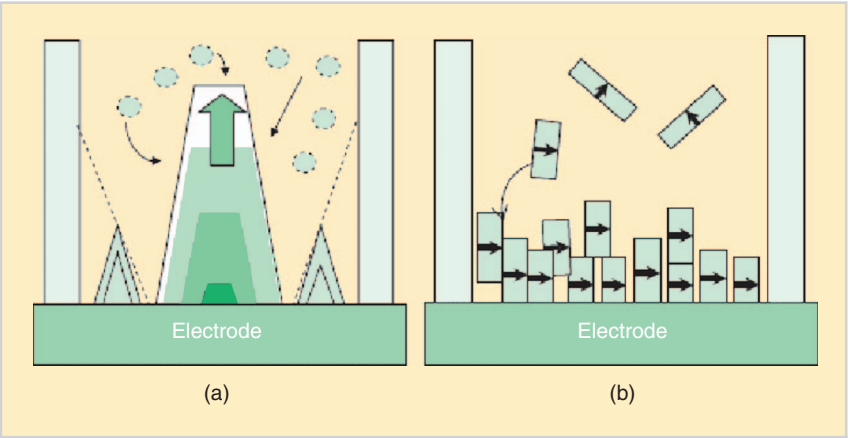

FIGURE 2 Schematic illustrations of growth mechanisms of single crystalline nanorods: (a) evolution selection growth and (b) homoepitaxial aggregation.

a single V_2O_5 nanorod, in which lattice fringes are clearly visible. The spacing of the fringes was measured to be 0.207 nm for nanorod grown from route A, and 0.208 nm for nanorod made from V_2O_5 sol. These values are similar for different synthesis route and correspond well with the spacing of (202) planes at 0.204 nm. These fringes make an angle of 88.9° with the long axis of the nanorod, which is consistent with a growth direction of [010].

Similar measurements made on high-resolution images of other nanorods also yield results consistent with a [010] growth direction. The formation of single-crystal nanorods from solutions by electrochemical deposition is attributed to evolution selection growth [Figure 2(a)]. The initial heterogeneous nucleation or deposition on the substrate surface results in the formation of nuclei with random orientation. The subsequent growth of various facets of a nucleus is dependent on the surface energy and varies significantly from one facet to another [22]. In the case of nanorods made from the V_2O_5 sol by electrophoretic deposition, the formation of single-crystal nanorods is explained by homoepitaxial aggregation of crystalline nanoparticles [Figure 2(b)]. Thermodynamically, it is favorable for the crystalline nanoparticles to aggregate epitaxially; such growth behavior and mechanism have been well reported in literature [23]. As a result, V_2O_5 nanorods grown by electrochemical deposition from solutions are dense single crystals, whereas the nanorods grown from sol electrophoresis are also single crystalline but have many defects inside the crystal. Such difference in nanostructure determines the different electrochemical behavior of nanorods grown from different solutions or sol. The nanorods grown from V_2O_5 sol by electrophoresis show the best kinetic property for Li-ion intercalation. All the V_2O_5 nanorod arrays show higher capacity and enhanced rate capability in comparison with the sol–gel derived polycrystalline V_2O_5 film. For example, the V_2O_5 nanorod arrays grown from VO^{2+} solution deliver five times the capacity of the film at a current density of 0.7 A/g. For the single-crystal nanorod arrays, the long axis (growth direction) is parallel to the interlayers of V_2O_5, thus the nanorods provide shorter and simpler diffusion path for Li ions and allow the most freedom for dimension change.

Using the similar template-based electrodeposition method but with different growth conditions, Wang et al. prepared nanotube arrays of $V_2O_5 \cdot nH_2O$ [24]. The authors found that nanotubes resulted when using lower voltage and shorter deposition time compared with the conditions for preparing nanorods. The $V_2O_5 \cdot nH_2O$ nanotube arrays demonstrate an initial high capacity of 300 mAh/g, about twice the initial capacity of 140 mAh/g from the $V_2O_5 \cdot nH_2O$ film. Such enhancement of capacity is due to the large surface area and short diffusion distances offered by the nanotube array. Subsequently, the authors used a two-step electrodeposition method to prepare Ni-$V_2O_5 \cdot nH_2O$ core–shell nanocable arrays [25]. Ni nanorod arrays were first grown by the template-based electrochemical deposition. In the second step, the hydrated vanadium pentoxide shell was deposited onto the surface of nickel nanorods through sol electrophoretic deposition. Figure 3 shows the scanning electron microscope (SEM) images of these three different nanostructures of vanadium oxides: V_2O_5 nanorod array, $V_2O_5 \cdot nH_2O$ nanotube array, and Ni-$V_2O_5 \cdot nH_2O$ core–shell nanocable array. Figure 4 compares the electrochemical performance of Ni-$V_2O_5 \cdot nH_2O$ nanocable arrays, single-crystal V_2O_5 nanorod arrays, and sol–gel derived V_2O_5 films.

Obviously Ni-$V_2O_5 \cdot nH_2O$ nanocable arrays demonstrate remarkably improved capacity and rate capability in comparison with the other two. The intercalation capacities of both nanorod arrays and sol–gel films decrease rapidly as the current density increases, while nanocable arrays are able to retain the high capacity at high current density (discharge rate), indicating the excellent

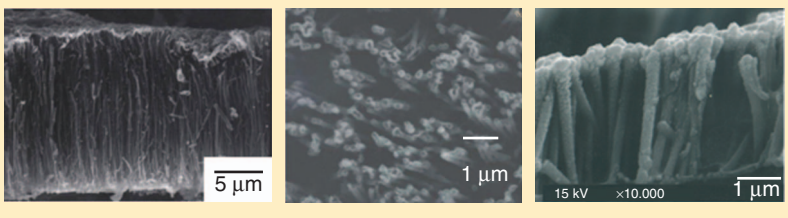

FIGURE 3 SEM images of (a) V_2O_5 nanorod array, (b) $V_2O_5 \cdot nH_2O$ nanotube array, and (c) Ni-$V_2O_5 \cdot nH_2O$ core–shell nanocable array.

high-rate performance of nanocable arrays. As shown in Figure 4(c), Ni-$V_2O_5 \cdot nH_2O$ nanocable array has significantly higher energy density and power density than those of the nanorod array and sol–gel film by at least one order of magnitude, which is ascribed to the enhanced surface area and reduced internal resistance.

OTHER VANADIUM OXIDE NANOSTRUCTURES

Following the systematic studies on ordered arrays of V_2O_5 nanorods, nanotubes, and nanocables, Lee et al. reported the synthesis and electrochemical properties of V_2O_5 films with nanosized features [26]. Typically, platelet and fibrillar structured V_2O_5 films were prepared by solution methods, and the discharge capacities and cyclic performance of these films were compared with those of the conventional plain structured film.

The platelet film consists of 20–30-nm sized standing platelets perpendicular to the substrate with random orientation, whereas fibrillar film is composed of randomly oriented nanofibers, though most of them protrude from the substrate surface. The initial discharge capacities of platelet and fibrillar structured V_2O_5 films are 1,240 and 720 mAh/g, respectively, which are far larger than the initial discharge value (260 mAh/g) of the plain structure film. Such large discharge capacity values are ascribed to the combined effects of the reduced Li^+ diffusion distance, which prevents concentration polarization of Li^+ in the V_2O_5 electrode and poor interlayered cross-linking offering more Li^+ intercalation. However, platelet and fibrillar structured V_2O_5 films were easily degraded during electrochemical cyclic tests. Similarly, platelet-structured V_2O_5 films are also obtained by dc sputtering but shows good cycling performance [27]. The capacity only changes from 80 to 73 μAh/cm^2 after 100 cycles and to 70 μAh/cm^2 after 200 cycles at a current density of 100 μAh/cm^2. These results can be explained by the *h00* preferred orientation of the film, which ensures a good homogeneity for

> Moving from bulk materials to the nanoscale can significantly change device performance for energy storage and conversion.

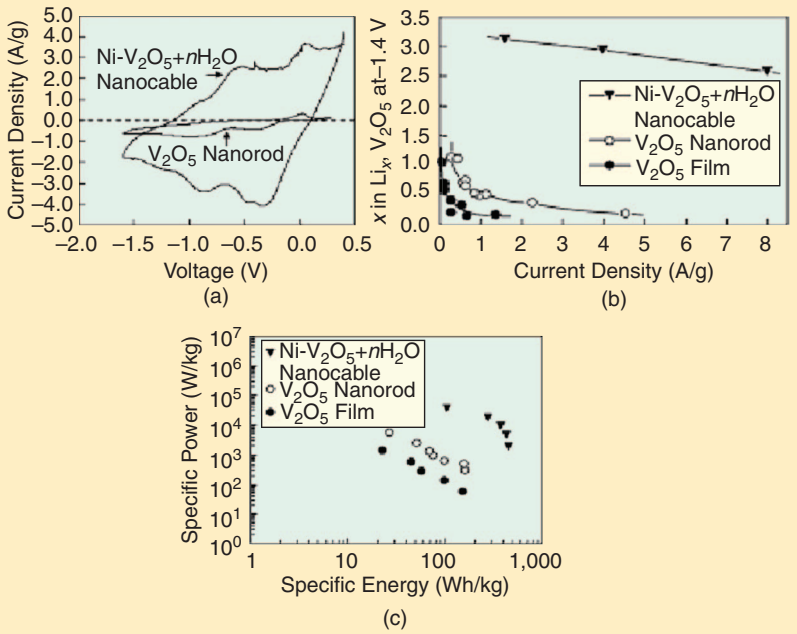

FIGURE 4 (a) Cyclic voltammograms of Ni-$V_2O_5 \cdot nH_2O$ nanocable array and V_2O_5 nanorod array using a scan rate of 10 mV/s. (b) Relationship between current density and Li intercalation capacity of Ni-$V_2O_5 \cdot nH_2O$ nanocable array, V_2O_5 nanorod array and sol–gel film from chronopotentiometric measurements. (c) Ragone plot for Ni-$V_2O_5 \cdot nH_2O$ nanocable array, V_2O_5 nanorod array, and sol–gel film.

Li intercalation or deintercalation and thus a good cyclability.

In addition to V_2O_5 thin films with structural features on the nanoscale, mesoporous vanadium oxides with nanometer-sized pores facilitate the diffusion of Li ions. Liu et al. synthesized mesoporous vanadium oxide with pore sizes ranging from 3 to 4 nm by electrodepositing from a $VOSO_4$ solution in the presence of a block polyalkylene oxide polymer (P123) [28]. This polymer surfactant plays a key role in the formation of mesoporous structure. The authors specifically investigated the rate performance of the mesoporous vanadium oxide electrode and found that the material delivered a capacity of 125 mAh/g at a high rate of 50 °C, corresponding to a capacitance of 450 F/g which is comparable to that of porous carbon capacitors. Therefore, the mesoporous vanadium oxide is very promising as cathode material for high-power Li-ion batteries and fills in the gap between batteries and capacitors. Moreover, the mesoporous structure provides elasticity that allows for dimensional change during Li-ion intercalation or deintercalation and, thus, offers good cyclability.

CONCLUSIONS

This article clearly reveals how moving from bulk materials to the nanoscale can significantly change device performance for energy storage and conversion. The development of high-performance Li-ion batteries can benefit from the distinct

properties of nanomaterials, such as high surface areas, short diffusion paths, and a large quantity of active sites, as well as freedom for volume change during charging or discharging cycles. Among a wide range of synthetic methods in preparing nanomaterials, simple and elegant are soft chemistry routes that involve sol–gel reactions and that frequently use organic molecules as structure-directing templates.

Applications of nanotechnology in energy storage are in the stage of research and development. For realization of wide industrial applications, further work is required to achieve controlled and large-scale synthesis of nanostructures, to understand mechanisms of Li storage in nanomaterials and kinetic transport on the interface between electrode and electrolyte. The effects of nanostructures in battery performance are not simple consequences of a reduction in size. The interfacial properties are subtle and critical, considering space–charge effects at the interface between nanosized electrode materials and charge transport between electrode and electrolyte. This challenges researchers worldwide to carry out systematic experimental studies and to develop predictive theoretical tools for better fundamental understanding of relationships between nanostructures and electrochemical characteristics of electrode materials.

ACKNOWLEDGMENTS

This work has been supported in part by National Science Foundation (DMI-0455994) and Air Office of Scientific Research (AFOSR-MURI, FA9550-06-1-032). This work has also been supported by the Center for Nanotechnology at the University of Washington (UW), Pacific Northwest National Laboratories (PNNL), Joint Institute of Nanoscience and Nanotechnology (JIN, UW, and PNNL), Washington Technology Center (WTC), and JFE Steel Corporation, Japan. Y. Wang would like to acknowledge the Ford, Nanotechnology, and JIN graduate fellowships. A portion of the research (TEM study) described in this article was performed in the Environmental Molecular Sciences Laboratory, a national scientific user facility sponsored by the Department of Energy's Office of Biological and Environmental Research and located at PNNL.

ABOUT THE AUTHORS

Ying Wang (ywang@me.lsu.edu) received her B.S. degree in chemical physics from the University of Science and Technology of China in 1997, an M.A. degree in chemistry from Harvard University in 1999, and a Ph.D. degree in materials science and engineering from the UW in 2006. She worked as a postdoc fellow of materials science at Northwestern University from 2006 to 2008. She is currently an assistant professor of mechanical engineering at Louisiana State University (LSU).

Guozhong Cao (gzcao@u.washington.edu) received his B.S. degree from East China University of Science and Technology, an M.S. degree from Shanghai Institute of Ceramics, and a Ph.D. degree from Eindhoven University of Technology in the Netherlands. Prior to joining the UW faculty in 1996, he worked briefly in the University of Twente, the University of Nijmegen (the Netherlands), and Advanced Materials Lab (University of New Mexico and Sandia National Lab). He is currently a Boeing-Steiner Professor of materials science and engineering at the UW.

REFERENCES

[1] J. M. Tarascon and M. Armand, "Issues and challenges facing rechargeable lithium batteries," *Nature*, vol. 414, no. 15, pp. 359–368, 2001.

[2] A. S. Aricò, P. Bruce, B. Scrosati, J.-M. Tarascon, and W. V. Schalkwijk, "Nanostructured materials for advanced energy conversion and storage devices," *Nat. Mater.,* vol. 4, no. 5, pp. 366–377, 2005.

[3] M. S. Whittingham, "Lithium batteries and cathode materials," *Chem. Rev.,* vol. 104, no. 10, pp. 4271–4302, 2004.

[4] M. S. Whittingham, Y. Song, S. Lutta, P. Y. Zavalij, and N. A. Chernova, "Exploring and exploiting molecular recognition using covalent chemistry under thermodynamic control," *J. Mater. Chem.,* vol. 15, no. 33, pp. 3362–3380, 2005.

[5] D. W. Murphy, P. A. Christian, F. J. DiSalvo, and J. V. Waszczak, "Lithium incorporation by vanadium pentoxide," *Inorg. Chem.,* vol. 18, no. 10, pp. 2800–2803, 1979.

[6] R. Nesper, M. E. Spahr, M. Niederberger, and P. Bitterli, "Nanotubes," Int. Patent Appl. PCT/CH97/00470, 1997.

[7] M. E. Spahr, P. Bitterli, R. Nesper, M. Müller, F. Krumeich, and H.-U. Nissen, "Redoxaktive nanoröhren aus vanadiumoxid," *Angew. Chem.,* vol. 110, no. 9, pp. 1339–1342, 1998.

[8] K. S. Pillai, F. Krumeich, H.-J. Muhr, M. Niederberger, and R. Nesper, "The first oxide nanotubes with alternating inter-layer distances," *Solid State Ionics,* vol. 141–142, pp. 185–190, May 2001.

[9] D. Pan, S. Zhang, Y. Chen, J. G. Hou, "Hydrothermal preparation of long nanowires of vanadium oxide," *J. Mater. Res.,* vol. 17, no. 8, pp. 1981–1984, 2002.

[10] U. Schlecht, M. Knez, V. Duppel, L. Kienle, and M. Burghard, "Boomerang-shaped VO_x belts: Twinning within isolated nanocrystals," *Appl. Phys. A,* vol. 78, no. 4, pp. 527–529, 2004.

[11] J. Liu, X. Wang, Q. Peng, and Y. Li, "Vanadium pentoxide nanobelts: Highly selective and stable ethanol sensor materials," *Adv. Mater.,* vol. 17, no. 6, pp. 764–767, 2005.

[12] X. K. Hu, D. K. Ma, J. B. Liang, S. L. Xiong, J. Y. Li, and Y. T. Qian, "$V_2O_5 \cdot nH_2O$ crystalline nanosheets: Hydrothermal fabrication and structure evolution," *Chem. Lett.,* vol. 36, no. 4, pp. 560–562, 2007.

[13] G. Li, S. Pang, L. Jiang, Z. Guo, and Z. Zhang, "Environmentally friendly chemical route to vanadium oxide single-crystalline nanobelts as a cathode material for lithium-ion batteries," *J. Phys. Chem. B,* vol. 110, no. 19, pp. 9383–9386, 2006.

[14] B. Li, Y. Xu, G. Rong, M. Jing, and Y. Xie, "Vanadium pentoxide nanobelts and nanorolls: From controllable synthesis to investigation of their electrochemical properties and photocatalytic activities," *Nanotechnology,* vol. 17, no. 10, pp. 2560–2566, 2006.

[15] C. K. Chan, H. Peng, R. D. Tweten, K. Jarausch, X. F. Zhang, and Y. Cui, "Fast, completely reversible Li insertion in vanadium pentoxide nanoribbons," *Nano Lett.,* vol. 7, no. 2, pp. 490–495, 2007.

[16] C. J. Patrissi and C. R. Martin, "Sol-gel-based template synthesis and Li-insertion rate performance of nanostructured vanadium pentoxide," *J. Electrochem. Soc.,* vol. 146, no. 9, pp. 3176–3190, 1999.

[17] N. Li, C. J. Patrissi, and C. R. Martin, "Rate capabilities of nanostructured $LiMn_2O_4$ electrodes in aqueous electrolyte," *J. Electrochem. Soc.,* vol. 147, no. 6, pp. 2044–2049, 2000.

[18] C. R. Sides and C. R. Martin, "Nanostructured electrodes and the low-temperature performance of Li-ion batteries," *Adv. Mater.,* vol. 17, no. 1, pp. 125–128, 2005.

[19] K. Takahashi, S. J. Limmer, Y. Wang, and G. Z. Cao, "Synthesis and electrochemical properties of single-crystal V_2O_5 nanorod arrays by template-based electrodeposition," *J. Phys. Chem. B,* vol. 108, no. 28, pp. 9795–9800, 2004.

[20] K. Takahashi, S. J. Limmer, Y. Wang, and G. Z. Cao, "Growth and electrochemical properties of single-crystalline V_2O_5 nanorod arrays," *Jpn. J. Appl. Phys.,* vol. 44, no. 1B, pp. 662–668, 2005.

[21] K. Takahashi, Y. Wang, and G. Z. Cao, "Growth and electrochromic properties of single-crystal V_2O_5 nanorod arrays," *Appl. Phys. Lett.,* vol. 86, no. 5, p. 053102, 2005.

[22] A. van der Drift, "Evolutionary selection: A principle governing growth orientation in vapour-deposited layers," *Philips Res. Rep.,* vol. 22, pp. 267–288, 1968.

[23] R. L. Penn and J. F. Banfield, "Morphology development and crystal growth in nanocrystalline aggregates under hydrothermal conditions: Insights from titania," *Geochim. Cosmochim. Acta,* vol. 63, no. 10, pp. 1549–1557, 1999.

[24] Y. Wang, K. Takahashi, H. Shang, and G. Z. Cao, "Synthesis and electrochemical properties of vanadium pentoxide nanotube arrays," *J. Phys. Chem. B,* vol. 109, no. 8, pp. 3085–3088, 2005.

[25] K. Takahashi, Y. Wang, and G. Z. Cao, "Ni-$V_2O_5 \cdot nH_2O$ core–shell nanocable arrays for enhanced electrochemical intercalation," *J. Phys. Chem. B,* vol. 109, no. 1, pp. 48–51, 2005.

[26] K. Lee, Y. Wang, and G. Z. Cao, "Dependence of electrochemical properties of vanadium oxide films on their nano- and microstructures," *J. Phys. Chem. B,* vol. 109, no. 35, pp. 16700–16704, 2005.

[27] C. Navone, R. Baddour-Hadjean, J. P. Pereira-Ramos, and R. Salot, "High-performance oriented V_2O_5 thin films prepared by DC sputtering for rechargeable lithium microbatteries," *J. Electrochem. Soc.,* vol. 152, no. 9, pp. A1790–A1796, 2005.

[28] P. Liu, S. Lee, E. Tracy, Y. Yan, and J. A. Turner, "Preparation and lithium insertion properties of mesoporous vanadium oxide," *Adv. Mater.,* vol. 14, no. 1, pp. 27–30, 2002.